

# Nuclear magnetic relaxation of $^{119}\text{Sn}$ , $^{35}\text{Cl}$ , and $^{127}\text{I}$ in two symmetric top molecules, $\text{SnCl}_3\text{I}$ and $\text{SnI}_3\text{Cl}$ , in liquid mixtures

Robert R. Sharp and John W. Tolan\*

Department of Chemistry, University of Michigan, Ann Arbor, Michigan 48104  
(Received 30 June 1975)

$^{119}\text{Sn}$  nuclear magnetic relaxation times were measured for the two symmetric top chloriodides of tin in the liquid state using pulsed nuclear magnetic resonance. The temperature and magnetic field dependence of  $T_1$  and  $T_2$  of  $^{119}\text{Sn}$  in  $\text{SnCl}_3\text{I}$  and  $\text{SnI}_3\text{Cl}$  were studied to identify and separate relaxation mechanisms. The longitudinal relaxation rates were found to arise from competing scalar and spin-rotation interactions, while the transverse rates are completely scalar dominated.  $T_1$ 's of both  $\text{SnCl}_3\text{I}$  and  $\text{SnI}_3\text{Cl}$  show evidence of a maximum in  $(T_1)_{\text{scalar}}^{-1}$  when  $T_2(^{127}\text{I})$  equals the difference of the  $^{119}\text{Sn}$  and  $^{127}\text{I}$  Larmor frequencies. This behavior is predicted by Abragam's "scalar relaxation of the second kind." The maximum occurs near the melting points in a 5 kG field and was used indirectly to determine  $^{127}\text{I}$  relaxation times. A least-squares analysis of these results permitted direct determination of three tin-halogen scalar coupling constants:  $J(^{119}\text{Sn}-^{127}\text{I}) = 1638$  Hz for  $\text{SnCl}_3\text{I}$ ,  $J(^{119}\text{Sn}-^{127}\text{I}) = 1097$  Hz for  $\text{SnI}_3\text{Cl}$ , and  $J(^{119}\text{Sn}-^{35}\text{Cl}) = 421$  Hz for  $\text{SnI}_3\text{Cl}$ . Rotational correlation times and halogen relaxation times were also measured as a function of temperature. The analysis failed to reveal a  $T_1$  component due to chemical shift anisotropy for any of the compounds at or below 13.3 kG. A comparison of molecular rotational correlation times with those of the unmixed tetrahalides,  $\text{SnCl}_4$  and  $\text{SnI}_4$ , indicates that electric dipole forces and shape effects associated with deviations from tetrahedral symmetry are less important determinants of the rotational diffusion tensor than is intermolecular rotational friction resulting from London dispersion forces. The effect on rotational diffusion constants of varying the composition of the medium was examined and found to be small.

## INTRODUCTION

Nuclear relaxation of  $^{119}\text{Sn}$  has previously been studied in the pure liquid tetrahalides  $\text{SnCl}_4$ ,  $\text{SnBr}_4$ , and  $\text{SnI}_4$ .<sup>1</sup> Relaxation in the latter two liquids is quite unusual, in that scalar coupling between directly bonded tin and halogen isotopes is a very efficient relaxation pathway both for spin-spin and spin-lattice relaxation. In the present paper, scalar relaxation times and the information they contain are examined in two symmetric top molecules,  $\text{SnCl}_3\text{I}$  and  $\text{SnI}_3\text{Cl}$ , by means of variable field and variable temperature measurements on the  $^{119}\text{Sn}$  resonance.

In the covalent tin tetrahalides, the two magnetic isotopes of tin,  $^{117,119}\text{Sn}$ , are spin  $\frac{1}{2}$  and are strongly scalar coupled to the halogen isotopes, all of which possess quadrupole moments ( $^{35,37}\text{Cl}$  and  $^{79,81}\text{Br}$  are spin  $\frac{3}{2}$ ,  $^{127}\text{I}$  is spin  $\frac{5}{2}$ ). This scalar coupling is not static, but is modulated rapidly in time by relaxation of the halogens, for which  $T_1$  is of the order  $(0.05-50) \times 10^{-6}$  sec. Rapid relaxation of the halogens produces random fluctuation in precessional angular velocity of  $^{119}\text{Sn}$  and results in line broadening of the tin resonances, or equivalently a shortening of  $T_2$ . Rapidly modulated scalar coupling also provides a mechanism for energy exchange between  $^{119}\text{Sn}$  and the thermal reservoir and thereby also shortens  $T_1$ . However, in the vast majority of cases involving light nuclei (e.g.,  $^1\text{H}$  or  $^{13}\text{C}$ ), scalar contributions to  $T_1$  are undetectable since they are orders of magnitude smaller than contributions due to other mechanisms, such as magnetic dipole coupling. Scalar  $T_1$ 's are proportional to the spectral density of the scalar interaction at the Larmor difference frequency  $(\omega_I - \omega_S)$  of the coupled spins. Scalar coupling is an efficient  $T_1$  mechanism only when the relaxation time of the  $S$  spin is very short ( $\lesssim 10^{-5}$  sec) and the coupling constant is very large.

These conditions are satisfied when tin or other heavy metals are directly bonded to bromine or iodine. The theory of scalar relaxation has been developed by Abragam<sup>2</sup> and leads to the following expressions:

$$(T_2)_{\text{SC}}^{-1} = \frac{1}{3} A^2 S(S+1) \left\{ T_{1S} + \frac{T_{2S}}{1 + (\omega_I - \omega_S)^2 T_{2S}^2} \right\}, \quad (1a)$$

$$(T_1)_{\text{SC}}^{-1} = \frac{2}{3} A^2 S(S+1) \left\{ \frac{T_{2S}}{1 + (\omega_I - \omega_S)^2 T_{2S}^2} \right\}. \quad (1b)$$

$A = 2\pi J$  is the scalar coupling constant and  $T_{1S} = T_{2S}$  is the relaxation time of quadrupolar spin  $S$ . From these expressions it is evident that  $T_{1, \text{SC}} = T_{2, \text{SC}}$  in the low field limit, and that  $T_{1, \text{SC}}$  and  $T_{2, \text{SC}}$  are unequal and field dependent outside this limit. The functional dependence of scalar relaxation is shown in Fig. 1.  $T_{1, \text{SC}}$  is seen to pass through a minimum with increasing temperature at constant field. At temperatures above the minimum,  $T_{1, \text{SC}}$  approaches asymptotically a proportionality with the square of the magnetic field strength, while at temperatures below the minimum,  $T_{1, \text{SC}}$  becomes field independent.

When scalar components can be identified through variable field measurements of both  $T_1$  and  $T_2$ , Eqs. (1) provide a straightforward method for determining scalar coupling constants and halogen relaxation times. In this way, the extremely short relaxation times of  $^{127}\text{I}$  and  $^{79,81}\text{Br}$  in  $\text{SnI}_4$  and  $\text{SnBr}_4$  were obtained from studies of the  $^{119}\text{Sn}$  relaxation. It is also well known that relaxation rates of quadrupolar isotopes are directly proportional to correlation times for molecular reorientation, and can be used to compute rotational diffusion coefficients when the relevant quadrupole coupling constants are known. Thus the relaxation of  $^{119}\text{Sn}$  provided an indirect, but unambiguous means for studying reorientational molecular motion in the liquid tin tetrahalides.

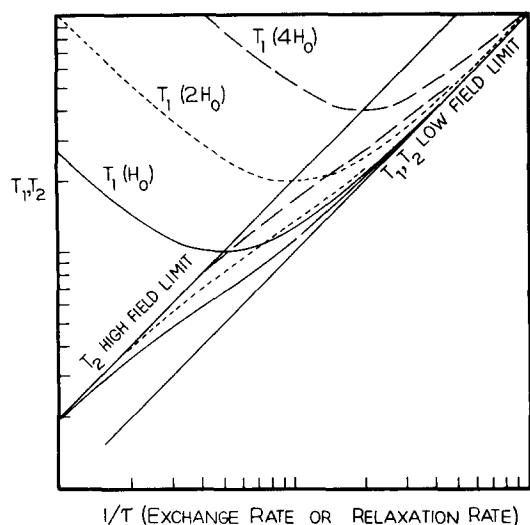


FIG. 1. The functional dependence of scalar relaxation times on the magnetic field strength  $H_0$  and the correlation time for scalar coupling  $\tau$ . Physically,  $\tau$  may be the lifetime of a nucleus in one site in a chemical exchange process (scalar relaxation of the first kind) or it may be the nuclear relaxation time of a quadrupolar nucleus (scalar relaxation of the second kind).

In view of these previous experiments we felt that a comparative study of the mixed tin chloriodides of symmetric top symmetry,  $\text{SnCl}_3\text{I}$  and  $\text{SnI}_3\text{Cl}$ , would provide interesting information about nuclear spin interactions and about molecular reorientation. However, an assignment of relaxation mechanisms is less simple for these molecules than for the unmixed tetrahalides since scalar coupling to two different halogens contributes to the metal relaxation. Furthermore, as shown by Eqs. (1a)–(1b),  $T_2$  tends to reflect primarily scalar coupling to the more slowly relaxing halogen, ( $^{35,37}\text{Cl}$ ), while  $(T_1)_{sc}^{-1}$  is usually controlled by the halogen with the shorter  $T_2$ , ( $^{127}\text{I}$ ). Thus a separation of relaxation components arising from scalar coupling of  $^{119}\text{Sn}$  to specific halogen isotopes may be difficult to achieve, and a determination of  $A(\text{Sn}-\text{X})$  and  $T_2(\text{X})$  based solely on the metal relaxation times is not in general possible. Fortunately, the relaxation times of  $^{35,37}\text{Cl}$  are sufficiently long to be measured directly while those of  $^{127}\text{I}$  are sufficiently short that  $T_{1,sc}$  is in the region of the minimum shown in Fig. 1. In this region  $T_{1,sc}$ , as well as  $T_{2,sc}$ , can be separated unambiguously from the temperature and field dependence of the  $T_1$  data alone. A computer fit of  $(T_1)_{sc}^{-1}$  to the functional form of Eq. (1b) thus determines  $T_2(^{127}\text{I})$  and  $A(^{119}\text{Sn}-^{127}\text{I})$  quite satisfactorily. To the best of our knowledge this theoretically predicted minimum in  $T_{1,sc}$  has never previously been observed, but it is a general feature of relaxation in the tin iodides at sufficiently low magnetic fields ( $H_0 \approx 2.5$  kG).

A knowledge of the halogen relaxation times in  $\text{SnCl}_3\text{I}$  and  $\text{SnI}_3\text{Cl}$  provides a useful probe of molecular reorientation of these molecules. Rotational motion of the symmetric tops,  $\text{SnCl}_3\text{I}$  and  $\text{SnI}_3\text{Cl}$ , is compared with that of the spherical tops,  $\text{SnCl}_4$  and  $\text{SnI}_4$ , in the same mixtures. Since the symmetric tops possess substantial dipole moments and lack tetrahedral symmetry, this comparison provides a means of assessing the influence of these fac-

tors on rotational diffusion constants. The tin chloriodides provide a particularly interesting series for comparison, since  $\text{SnCl}_4$  and  $\text{SnI}_4$  have as nearly spherical potential energy profiles as is likely to be found for polyatomic molecules.

The mixed tetrahalides of tin have been the subject of several vibrational spectroscopy studies.<sup>3,4</sup> NMR resonances of the mixed species were first observed by Burke and Lauterbur in their study of the redistribution reactions of  $\text{Sn}(\text{IV})$  halides.<sup>5</sup> When two pure tin tetrahalides are mixed, chemical exchange reactions occur which result in a nearly random distribution of all the mixed tetrahalides. These exchange processes are slow on the NMR time scale since well separated resonances, broadened by scalar coupling to the halogens, were observed for each of the species. The resonance positions of  $\text{SnX}_4$  and  $\text{SnY}_4$  are unchanged from those in the neat liquids. Chemical shifts of  $\text{SnCl}_4$ ,  $\text{SnBr}_4$  and  $\text{SnI}_4$  are to high field of tetramethyl tin by 150, 638 and 1698 ppm respectively, and the chemical shifts of mixed halides appear at nearly equally spaced intermediate intervals. Burke and Lauterbur used different ratios of  $\text{SnX}_4$ : $\text{SnY}_4$  to confirm the assignment of the resonances. Relative concentrations of the various species were measured from intensities of  $^{119}\text{Sn}$  resonances to verify that the distribution of halogen atoms is indeed random. Figure 2 shows the percentage of each  $\text{MX}_n\text{Y}_{4-n}$  component in such a  $\text{MX}_4 + \text{MY}_4$  mixture, assuming random distribution, versus the mole fraction of  $\text{MX}_4$  and  $\text{MY}_4$  before mixing.

## EXPERIMENTAL

Reagent Grade  $\text{SnCl}_4$ ,  $\text{SnBr}_4$ , and  $\text{SnI}_4$  (Alpha Inorganics) were used without further purification to prepare liquid mixtures of the tin tetrahalides. Samples were prepared by weight in approximately 3:1 mole ratios; that is, each  $\text{SnX}_4$  and  $\text{SnY}_4$  pair was combined in 3:1 and 1:3 mole ratios in order to maximize the concentration of the symmetric top  $\text{SnX}_3\text{Y}$  and  $\text{SnXY}_3$  molecules as shown in Fig. 1. Concentrations of the different species are approximately 30%  $\text{SnX}_4$ , 43%  $\text{SnX}_3\text{Y}$ , 20%  $\text{SnX}_2\text{Y}_2$ , and less than 5% each of  $\text{SnXY}_3$  and  $\text{SnY}_4$ . All samples were degassed by successive freeze-pump-thaw cycles until bubbles ceased to evolve during thawing.

Relaxation times were measured using a pulsed appa-

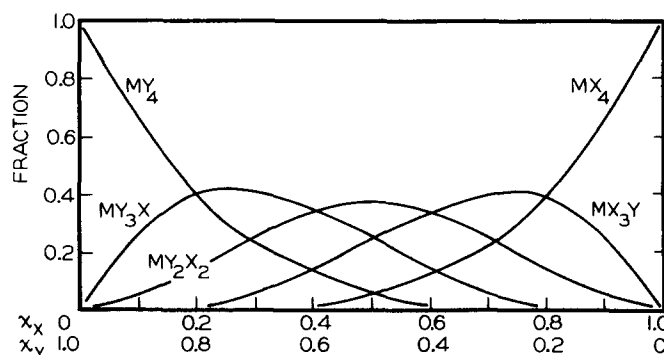


FIG. 2. The fractions, of  $\text{MX}_n\text{Y}_{4-n}$  components in a  $\text{MX}_4 + \text{MY}_4$  mixture assuming random distribution of X and Y.

ratus described elsewhere.<sup>1,6</sup>  $T_1$  was measured from a semilog plot of signal height of the free induction decay following the  $90^\circ$  pulse in a  $180-\tau-90$  sequence.  $T_1$ 's were initially estimated using the null method in order that an interval of  $5 T_1$  could be inserted between pulse sequences.  $T_2$  was measured using the phase-shifted Carr-Purcell sequence. Again, an off time of  $5 T_1$  was inserted between sequences, and the sequence duration was set at approximately  $10 T_2$  to establish a reliable baseline. Measurements of  $T_2$  were made at Carr-Purcell pulse spacings of 0.4, 0.6, and 0.8 msec, with no systematic variation in  $T_2$  seen among them.

Some  $T_1$  measurements of  $^{119}\text{Sn}$  in  $\text{SnCl}_4$ ,  $\text{SnBr}_4$  and  $\text{SnI}_4$  have recently been reported by Lassigne,<sup>7</sup> who used a Fourier transform spectrometer operating at 25.1 kG. Lassigne's data are in excellent agreement with our earlier results.

The  $^{35}\text{Cl}$  relaxation time of  $\text{SnI}_3\text{Cl}$  was determined directly from the free induction decay of the  $^{35}\text{Cl}$  resonance. The measurement was made at 8.227 MHz (19.7 kG), with a sample temperature of  $375^\circ\text{K}$ .  $T_2$  is quite short ( $\sim 25 \mu\text{sec}$ ) and somewhat less than the spectrometer dead time even at relatively high temperature. The dead time was minimized by attaching a  $100 \Omega$  metal film resistor across the probe transmitter coil, lessening its "Q." In addition, a nutating pulse of about  $60^\circ$  was chosen, which gives good signal amplitude with significantly reduced dead time.

Since the acquisition time of the Fabritek CAT is about  $50 \mu\text{sec}$ , direct accumulation of the signals was not possible. A special interface was constructed to sample and integrate the signal during a  $10 \mu\text{sec}$  window that is digitally stepped along the F. I. D. starting at the end of the dead period. The window chosen is not negligible in duration compared to the measured  $T_2$ , but straightforward integration shows that the integration signal is exponential in form with a time constant equal to the true  $T_2$ , irrespective of the window length. The window was automatically stepped along the F. I. D. at  $2 \mu\text{sec}$  intervals by a digitally controlled delay pulse derived from the B channel logic circuitry of the Bruker spectrometer. At each position along the F. I. D., the signal is sampled and integrated 512 times. In order to further improve the signal-to-noise ratio, the integral is held between successive sampling pulses and reset immediately before the opening of the sampling window. In this way the output of the integrator can be filtered with a time constant  $\tau \approx 0.1 \text{ sec}$  and fed directly to the CAT. Figure 3 shows the filtered output during a single sweep over the F. I. D. of neat  $\text{SnCl}_4$  at  $365^\circ\text{K}$ . The measured  $T_2$  is  $40 \pm 2 \mu\text{sec}$ , which compares very well with a literature value of  $39.0 \mu\text{sec}$ , obtained from a wide-line measurement at  $298^\circ\text{K}$ <sup>8</sup> combined with the measured activation energy ( $E_A = 1.86 \text{ kcal/mole}^1$ ) for  $T_2$ .

A sample made up from 18%  $\text{SnCl}_4$  and 82%  $\text{SnI}_4$  was used to determine  $T_2$  ( $^{35}\text{Cl}$ ) in  $\text{SnI}_3\text{Cl}$ . As seen from Fig. 2 the only chlorine-containing species present in significant quantities in this mixture are  $\text{SnI}_3\text{Cl}$  and  $\text{SnI}_2\text{Cl}_2$ , the former being 3.2 times as concentrated as the latter. The  $^{35}\text{Cl}$  free induction decay was measured with signal averaging as is shown in Fig. 3. A least-squares com-

puter fit of the data to an exponential decay converged to the curve shown in the figure. The best-fit  $T_2$  is  $23 \pm 4 \mu\text{sec}$ . The assumption is made that this relaxation is entirely due to the dominant  $\text{SnI}_3\text{Cl}$  species.

## OBSERVATION OF THE $^{119}\text{Sn}$ RESONANCES

The various contributions to the observed  $^{119}\text{Sn}$  relaxation data were separated according to their temperature and field dependence. The transverse relaxation rates  $(T_2)^{-1}$  were much more rapid than the corresponding longitudinal rates  $(T_1)^{-1}$ , which indicates that scalar relaxation dominates the transverse relaxation. Furthermore, the temperature dependence of  $(T_2)^{-1}$  indicates that this relaxation is due to scalar coupling modulated by the rapid quadrupolar relaxation of the directly bonded halogen atoms, rather than by chemical exchange.

Since  $(T_2)_{\text{SC}}^{-1} \gg (T_1)_{\text{SC}}^{-1}$ , the contributions of the chlorine isotopes can be described by a single equation of the form (1b):

$$(T_2)_{\text{SC}}^{-1} \cong (T_2)_{\text{SC}}^{-1} - \frac{1}{2} (T_1)_{\text{SC}}^{-1} \\ = \sum_{i=1,2} \frac{1}{3} X_i N S(S+1) A_i^2 \tau_i \left( \frac{\gamma_i}{\gamma_1} \right)^2 \left( \frac{Q_i}{Q_1} \right)^2. \quad (2a)$$

Thus,

$$(T_2)_{\text{Sn-Cl}}^{-1} = 50.8 N (A_{35}/2\pi)^2 \tau_{35} \quad (2b)$$

and

$$(T_2)_{\text{Sn-I}}^{-1} = 2.917 N (A_{127}/2\pi)^2 \tau_{127} \quad (2c)$$

for coupling to  $N$  chlorine and iodine nuclei, respectively.

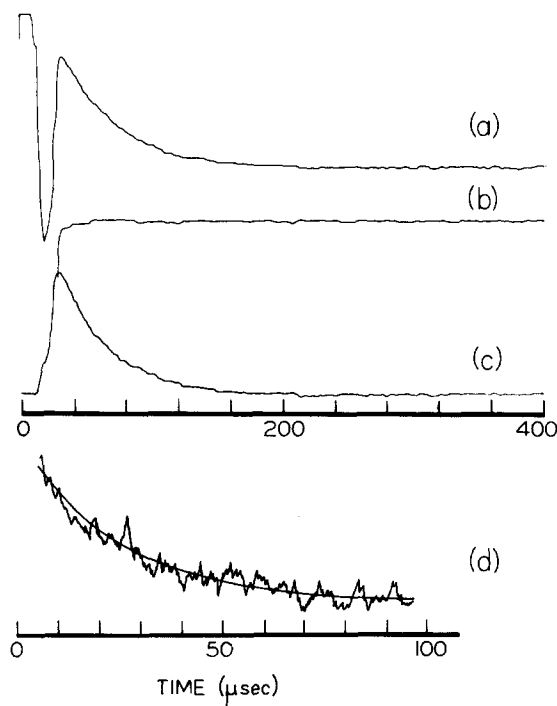


FIG. 3. Free induction decays of  $^{35}\text{Cl}$  measured at  $375^\circ\text{K}$ ; (a) neat  $\text{SnCl}_4$ , single scan (b) off-resonance baseline (c) neat  $\text{SnCl}_4$  with baseline subtracted (d)  $\text{SnI}_3\text{Cl}$  in the liquid mixture; solid line is a least squares fit of an exponential function to the data.

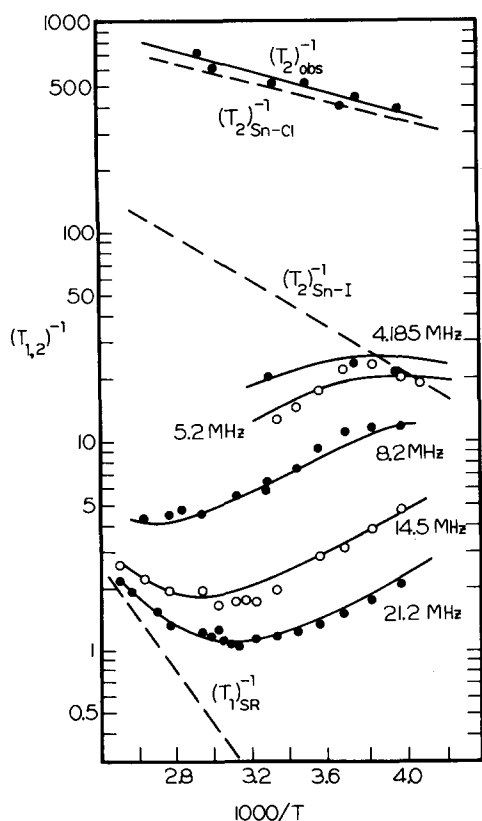


FIG. 4.  $(T_1)^{-1}$  and  $(T_2)^{-1}$  vs  $(1000/T)$  for  $^{119}\text{Sn}$  in  $\text{SnCl}_3\text{I}$  at several magnetic field strengths. Various mechanistic contributions are indicated by dashed lines. Solid lines are least squares curves fit to the data using theoretical expressions described in the text.

Longitudinal relaxation results in general from four competing mechanisms

$$(T_1)_{\text{obs}}^{-1} = (T_1)_{\text{SR}}^{-1} + (T_1)_{\text{SC}}^{-1} + (T_1)_{\text{d-d}}^{-1} + (T_1)_{\text{CSA}}^{-1}$$

where subscripts indicate components due to the spin-rotation interaction, scalar coupling, internuclear magnetic dipole coupling, and chemical shift anisotropy. Dipolar coupling was found to be negligible for the unmixed tin tetrahalides<sup>1</sup> and is unquestionably negligible also for the mixed tetrahalides. The other three mechanisms show qualitatively different behavior with variation of temperature and magnetic field and can be separated experimentally on the basis of this difference.  $T_1$ 's which decreases with increasing temperature, and which are field independent, are characteristic of the spin-rotation mechanism.  $(T_1)_{\text{SC}}^{-1}$  and  $(T_1)_{\text{CSA}}^{-1}$  are field dependent mechanisms, and both contributions normally increase with decreasing temperature.  $(T_1)_{\text{CSA}}^{-1}$  varies with the square of magnetic field strength  $H_0$ , and is given in symmetric top symmetry by (2)

$$(T_1)_{\text{CSA}}^{-1} = \frac{2}{15} \gamma^2 H_0^2 (\sigma_{\parallel} - \sigma_{\perp})^2 \tau_c$$

$\tau_c$  is the rotational correlation time for the unique axis and  $(\sigma_{\parallel} - \sigma_{\perp})$  is the shielding anisotropy. Scalar contributions to  $(T_1)^{-1}$  depend upon magnetic field strength in the manner described by Eq. (1b) and Fig. 1, and in most experimental circumstances vary as the inverse square of magnetic field strength. Using the same approxima-

tions that pertain to Eqs. (2a)–(2c), the contributions to  $(T_1)_{\text{SC}}^{-1}$  due chlorine and iodine can be written

$$(T_1)_{\text{Sn-Cl}}^{-1} = \frac{(3.89)NA_{35}^2}{\omega_{119}^2 \tau_{35}}, \quad (3a)$$

$$(T_1)_{\text{Sn-I}}^{-1} = \frac{(27.193)NA_{127}^2}{\omega_{119}^2 \tau_{127}}. \quad (3b)$$

These relations are invalid in the neighborhood of a maximum in  $(T_1)_{\text{SC}}^{-1}$ ; there the full functional dependence of Eqs. (1a) and (1b) must be used.

### $^{119}\text{SnCl}_3\text{I}$

$(T_1)^{-1}$  and  $(T_2)^{-1}$  for  $^{119}\text{Sn}$  in  $\text{SnCl}_3\text{I}$  and  $\text{SnI}_3\text{Cl}$  are shown as a function of temperature and magnetic field strength in Fig. 4 and are given in Table I.  $T_1^{-1}$  clearly passes through both a maximum and a minimum. At temperatures above the minimum the controlling relaxation mechanism is the spin-rotation interaction. This conclusion is confirmed from both the temperature dependence and the asymptotic field independence of the data. Below the minimum, the dominant interaction is scalar coupling as is evident from the approximate proportionality of  $(T_1)^{-1}$  with  $H_0^2$ . In principle, chemical shift anisotropy can also be important in this region, but a computer fit, which is discussed in more detail below, of the functional form of the data does not reveal an appreciable  $T_1$  component from this mechanism.

The  $^{119}\text{Sn}$  nucleus in  $\text{SnCl}_3\text{I}$  is scalar coupled to three halogen isotopes:  $^{35,37}\text{Cl}$  and  $^{127}\text{I}$ . The scalar portion of  $(T_1)^{-1}$  reflects entirely  $^{119}\text{Sn}$ – $^{127}\text{I}$  coupling, however, as is expected from the large difference in relaxation times of chlorine and iodine. An approximate value of  $(T_1)_{\text{SC,Cl}}^{-1}$  in  $\text{SnCl}_3\text{I}$  can be computed directly from Eq. (3a) using the measured value of  $T_2(^{35}\text{Cl})$  for  $\text{SnCl}_4$  in conjunction with the measured  $T_2(^{119}\text{Sn})$  in  $\text{SnCl}_3\text{I}$ , which is strongly dominated by scalar coupling to chlorine. The value computed in this manner is  $(T_1)_{\text{SC,Cl}}^{-1} = 3.9$  ( $10^{-4}$ ) $\text{sec}^{-1}$ , at  $298^\circ\text{K}$  and 10 kG, which confirms the relative insignificance of this contribution. Since chlorine scalar coupling is entirely negligible as a  $T_1$  mechanism, the remaining mechanisms can be separated quantitatively by fitting numerically  $(T_1)_{\text{obs}}^{-1}$  to an equation of the form

$$(T_1)_{\text{obs}}^{-1} = (T_1)_{\text{SR}}^{-1} + (T_1)_{\text{Sn-I}}^{-1} + (T_1)_{\text{CSA}}^{-1}$$

where

$$(T_1)_{\text{SR}}^{-1} = A \exp(-E_{\text{SR}}[1/RT - 1/RT_0]),$$

$$(T_1)_{\text{Sn-I}}^{-1} = B \tau / [1 + (\omega_{119} - \omega_{127})^2 \tau^2],$$

$$\tau = \tau_0 \exp(-E_{\text{SC}}[1/RT - 1/RT_0]).$$

and

$$(T_1)_{\text{CSA}}^{-1} = C(\omega_{119})^2 \tau.$$

An initial fit was achieved neglecting  $(T_1)_{\text{CSA}}^{-1}$ . Subsequently it was found that the fit could not be significantly improved by inclusion of a small term with the functional dependence of  $(T_1)_{\text{CSA}}^{-1}$ . This fitting procedure places a lower limit of about 7 sec on  $T_{1,\text{CSA}}$  at 13.36 kG and  $270^\circ\text{K}$ . The maximum in  $(T_1)_{\text{obs}}^{-1}$  is faithfully described by the functional form of  $(T_1)_{\text{Sn-I}}^{-1}$ . The three fitting parameters,  $B$ ,  $\tau_0$ , and  $E_{\text{SC}}$ , that describe the field and

TABLE I.  $^{119}\text{Sn}$  relaxation times in  $\text{SnCl}_3\text{I}$  as a function of temperature and magnetic field strength.

$H_0$	2.63 kG		3.28 kG		5.17 kG		9.14 kG		13.36 kG		9.14 kG	
$\nu(^{119}\text{Sn})$	4.185 MHz		5.20 MHz		8.20 MHz		14.50 MHz		21.20 MHz		14.5 MHz	
$\nu(^{127}\text{I})$	2.24 MHz		2.79 MHz		4.40 MHz		7.78 MHz		11.38 MHz		7.78 MHz	
	$T(^{\circ}\text{K})$	$T_1(\text{sec})$	$T(^{\circ}\text{K})$	$T_1(\text{sec})$	$T(^{\circ}\text{K})$	$T_1(\text{sec})$	$T(^{\circ}\text{K})$	$T_1(\text{sec})$	$T(^{\circ}\text{K})$	$T_1(\text{sec})$	$T(^{\circ}\text{K})$	$T_2(\text{sec})$
	251	0.047	243	0.053	249	0.081	249	0.22	249	0.50	249	0.025
	267	0.043	249	0.050	260	0.085	259	0.27	259	0.59	267	0.023
	303	0.049	259	0.045	269	0.088	269	0.32	269	0.69	270	0.024
			269	0.046	281	0.110	281	0.36	281	0.77	287	0.019
			281	0.058	292	0.133	302	0.52	291	0.82	301	0.019
			290	0.070	302	0.151	310	0.60	302	0.85	321	0.016
			302	0.078	302	0.164	315	0.58	310	0.89	336	0.014
					319	0.182	319	0.63	319	0.95		
					341	0.182	330	0.61	324	0.93		
					352	0.222	342	0.54	327	0.89		
					364	0.227	362	0.53	330	0.83		
					380	0.238	380	0.46	333	0.88		
							403	0.39	342	0.85		
									362	0.78		
									369	0.66		
									392	0.52		
									403	0.46		

temperature dependence of the scalar component of  $T_1$  permit a unique determination of the iodine relaxation time and the tin-iodine scalar coupling constant, since  $T_2(^{127}\text{I}) = \tau_0 \exp(-E_{\text{sc}}[1/RT - 1/RT_0])$  and  $A(^{119}\text{Sn}-^{127}\text{I}) = (2\pi J) = (B/5.83)^{1/2}$ . A coupling constant of 1638 Hz is found, which is 74% larger than the value for  $\text{SnI}_4$ . The  $^{127}\text{I}$  relaxation time varies between 0.5  $\mu\text{sec}$  at 144°C down to 0.07  $\mu\text{sec}$  at -18°C. Best values of the parameters obtained from the fitting procedure are given in Table III.

A mechanistic decomposition of the  $T_2$  data in terms of scalar contributions due to  $^{119}\text{Sn}-^{35,37}\text{Cl}$  and  $^{119}\text{Sn}-^{127}\text{I}$  coupling can be accomplished in a straightforward manner using the scalar coupling constant,  $A(^{119}\text{Sn}-^{127}\text{I})$ , and the iodine relaxation time determined from the  $T_1$  data. Using the values of  $A(^{119}\text{Sn}-^{127}\text{I})$ ,  $T_2(^{127}\text{I})$  and  $E_{\text{sc}}$  in Table III,  $(T_2)_{\text{Sn-I}}^{-1}$  can be computed as a function of temperature and is shown in Fig. 4. The tin-chlorine contribution,  $(T_2)_{\text{Sn-Cl}}^{-1}$ , is also plotted as the difference,  $(T_2)_{\text{obs}}^{-1} - (T_2)_{\text{Sn-I}}^{-1}$ .

Unfortunately, a direct measurement of the  $^{35}\text{Cl}$  relaxation time in  $\text{SnCl}_3\text{I}$ , which would give the tin-chlorine coupling constant, is difficult to obtain because of the necessarily large concentration of either  $\text{SnCl}_2\text{I}_2$  or  $\text{SnCl}_4$  in any mixture containing  $\text{SnCl}_3\text{I}$ . Even with good signal-to-noise ratios one must subtract away the unwanted contributions using an extrapolation procedure that accounts for relaxation during the pulse. If one uses the  $T_2$  of  $^{35}\text{Cl}$  in  $\text{SnCl}_4$  as an upper limit to that in  $\text{SnCl}_3\text{I}$ , an approximate value,  $A(^{119}\text{Sn}-^{35}\text{Cl}) \approx 378$  Hz, can be obtained for the  $^{119}\text{Sn}-^{35}\text{Cl}$  scalar coupling constant.

### $\text{SnI}_3\text{Cl}$

$T_1$  and  $T_2$  data for  $^{119}\text{SnI}_3\text{Cl}$  are given in Fig. 5 and Table II. Unlike  $^{119}\text{SnCl}_3\text{I}$ ,  $^{119}\text{SnI}_3\text{Cl}$  shows neither maximum nor minimum and is strongly dominated by  $^{119}\text{Sn}-$

$^{127}\text{I}$  scalar coupling throughout its temperature range. Although  $T_1$  is not observed to pass through a maximum, the curve at 4.18 MHz is quite near the maximum at temperatures just above the melting point. Both this curve and the one at 8.194 MHz deviate substantially from the simple  $H_0^2$  dependence that is observed when  $(\omega_{119} - \omega_{127})^2 T_2^2 \gg 1$ . At 370°C, for example,  $(T_1)_{\text{Sn-I}}^{-1}$  is 40% below the curve (shown as a fine dashed line in Fig. 5) that is predicted using the approximate expression

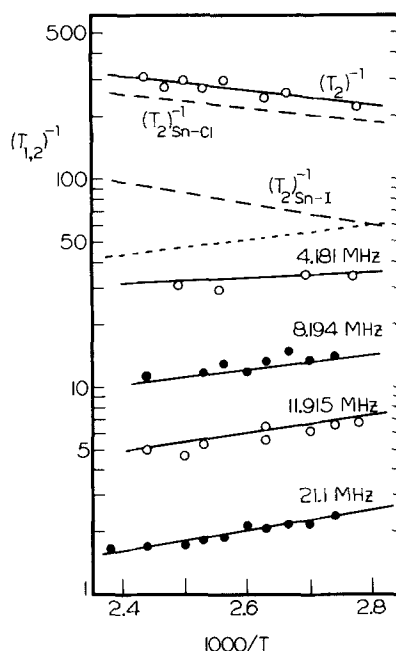


FIG. 5.  $(T_1)^{-1}$  and  $(T_2)^{-1}$  vs  $(1000/T)$  for  $^{119}\text{Sn}$  in  $\text{SnI}_3\text{Cl}$  at several magnetic field strengths. Solid lines are obtained from least squares computer fits described in the text. The finely dashed line is drawn to show the lowering of the data at 4.181 MHz due to proximity to the  $T_1$  minimum.

TABLE II.  $^{119}\text{Sn}$  relaxation times in  $\text{SnI}_3\text{Cl}$  as a function of temperature and magnetic field strength.

$H_0$	2.63 kG	5.16 kG	7.51 kG	13.30 kG	7.51 kG					
$\nu(^{119}\text{Sn})$	4.181 MHz	8.194 MHz	11.915 MHz	21.10 MHz	11.915 MHz					
$\nu(^{127}\text{I})$	2.24 MHz	4.79 MHz	6.40 MHz	11.33 MHz	6.40 MHz					
	$T(^{\circ}\text{K})$	$T_1(\text{sec})$	$T(^{\circ}\text{K})$	$T_1(\text{sec})$	$T(^{\circ}\text{K})$	$T_1(\text{sec})$	$T(^{\circ}\text{K})$	$T_1(\text{sec})$	$T(^{\circ}\text{K})$	$T_2(\text{msec})$
	361	0.029	365	0.070	360	0.147	364	0.41	360	4.0
	370	0.029	370	0.072	365	0.151	369	0.46	360	4.3
	391	0.034	373	0.066	369	0.154	375	0.48	372	3.9
	402	0.032	380	0.072	380	0.151	380	0.49	380	4.0
			391	0.076	380	0.175	385	0.49	390	3.4
			395	0.093	395	0.189	390	0.54	394	3.7
			410	0.089	399	0.182	395	0.56	400	3.3
					410	0.204	400	0.57	405	3.6
							410	0.60	410	3.2
							420	0.63		

(3b) and the high field data. Since the spin-rotation contribution is negligible,  $A(^{119}\text{Sn}-^{127}\text{I})$  and  $T_2(^{127}\text{I})$  can be computed from a simultaneous computer fit of  $(T_1)_{\text{obs}}^{-1}$  at all four frequencies to a three parameter expression of the form

$$(T_1)_{\text{Sn-I}}^{-1} = B \tau / [1 + (\omega_{119} - \omega_{127})^2 \tau^2] ,$$

$$\tau = \tau_0 \exp(-E_{\text{SC}}[1/RT - 1/RT_0]) .$$

Best-fit values for  $B$ ,  $\tau_0$ , and  $E_{\text{SC}}$  are given in Table III. Once again the inclusion of chemical shift anisotropy did not significantly improve the fit, which places an upper limit of approximately 5 sec on  $T_{1,\text{CSA}}$ .  $T_2(^{127}\text{I})$  is found to be  $0.124 \pm 0.020$  sec at  $400^\circ\text{K}$  from the least squares analysis.  $T_2(^{127}\text{I})$  lengthens with increasing temperature, exhibiting an activation energy of 2.3 kcal/mole. The fitting parameters  $B$  and  $\tau_0$  yield a  $^{119}\text{Sn}-^{127}\text{I}$  scalar coupling constant of 1097 Hz.

The scalar contributions to  $T_2$  arising from coupling to chlorine and iodine are readily computed from the results of the  $T_1$  analysis by means of Eq. (2c). Respective contributions are shown as dashed lines in Fig. 5. Making use also of the directly measured  $^{35}\text{Cl}$  relaxation time,  $T_2(^{35}\text{Cl}) = 23 \pm 4$   $\mu\text{sec}$  at  $375^\circ\text{K}$ , the magnitude of the  $^{119}\text{Sn}-^{35}\text{Cl}$  scalar coupling constant,  $A/2\pi = 421$  Hz, is obtained. The NMR parameters derived for both  $\text{SnCl}_3\text{I}$  and  $\text{SnI}_3\text{Cl}$  are summarized in Table III.

### ANISOTROPIC MOLECULAR REORIENTATION IN THE TIN CHLOROIODIDES

The halogen relaxation times obtained in the previous section provide a convenient probe of molecular reorientation in the tin chloroiodides. Relaxation of the halogen isotopes results from interactions between the nuclear electric quadrupole moment and electric field gradients arising from asymmetry in the surrounding electric charge distribution. From the theory of nuclear quadrupole relaxation<sup>2</sup> we have

$$(T_1)_Q^{-1} = \frac{3}{40} \{ (2I+3) / [I^2(2I-1)] \} (e^2qQ/\hbar)^2 \tau_Q , \quad (4)$$

where  $I$  is the halogen spin and  $e^2qQ/\hbar$  is the quadrupole coupling constant. The correlation time  $\tau_Q$  for this interaction is defined as the integral of the time correlation function for a second rank tensor fixed in the molec-

ular frame and is a direct measure of the time scale of molecular reorientation. In the limiting case where reorientation proceeds by a series of small angular steps, the motion is described by classical diffusion equations.<sup>9-11</sup> Thus an alternative parameter for describing reorientation is the rotational diffusion coefficient, which can be related to the integral of the angular velocity autocorrelation function<sup>10</sup>:

$$D_i = \int_0^\infty \langle \omega_i(0) \omega_i(t) \rangle dt . \quad (5)$$

According to Eq. (5),  $D_i$  describes the persistence of rotational motion about a given axis and is directly proportional to the correlation time  $\tau_J$  for molecular angular momentum:  $D_i = (kT/I_i) \tau_{Ji} = \langle \omega_i^2 \rangle \tau_{Ji}$ , where  $I$  is the moment of inertia about axis  $i$ , and  $\omega$  is the angular velocity of the free rotor. Hubbard<sup>11</sup> has also shown that the small-step assumption leads to the simple relation,  $D = \frac{1}{6} \tau_Q$ . More sophisticated theoretical models,<sup>12,13</sup> which will not be used here, are required to describe re-

TABLE III. Molecular and NMR parameters for  $\text{SnCl}_3\text{I}$  and  $\text{SnI}_3\text{Cl}$ .

	$\text{SnCl}_3\text{I}$	$\text{SnI}_3\text{Cl}$
$(e^2qQ/\hbar)(^{35}\text{Cl})$	46.92 MHz <sup>a</sup>	47.5 MHz <sup>a</sup>
$(e^2qQ/\hbar)(^{127}\text{I})$	1355 MHz <sup>a</sup>	1355 MHz <sup>a</sup>
$I_{\parallel} \times 10^{40}$	830.4 cgs <sup>b</sup>	3916.2 cgs <sup>b</sup>
$I_{\perp} \times 10^{40}$	1684.7 cgs <sup>b</sup>	2559.6 cgs <sup>b</sup>
$J(^{119}\text{Sn}-^{35}\text{Cl})$	(378 Hz) <sup>c</sup>	421 Hz
$J(^{119}\text{Sn}-^{127}\text{I})$	1638 Hz	1097 Hz
$\tau_0(\mu\text{sec})$	0.40 $\mu\text{sec}$	0.088 $\mu\text{sec}$
$T_0$	384.6 $^{\circ}\text{K}$	357 $^{\circ}\text{K}$
$E_{\text{SC}}$	2.5 kcal/mole	2.3 kcal/mole
$B$	0.618(10 <sup>9</sup> ) sec <sup>-2</sup>	0.864(10 <sup>9</sup> ) sec <sup>-2</sup>
$E_Q(T_2)$	1.0 kcal/mole	1.5 kcal/mole

<sup>a</sup>Computed from the correlation of Semin and Bryuchova, as described in the text.

<sup>b</sup>Computed assuming tetrahedral bond angles with bond distances equal to  $r_{\text{Sn-Cl}} = 2.30$   $\text{\AA}$  and  $r_{\text{Sn-I}} = 2.64$   $\text{\AA}$  (Ref. 25).

<sup>c</sup>Estimated using  $T_2(^{35}\text{Cl})$  for  $\text{SnCl}_4$ .

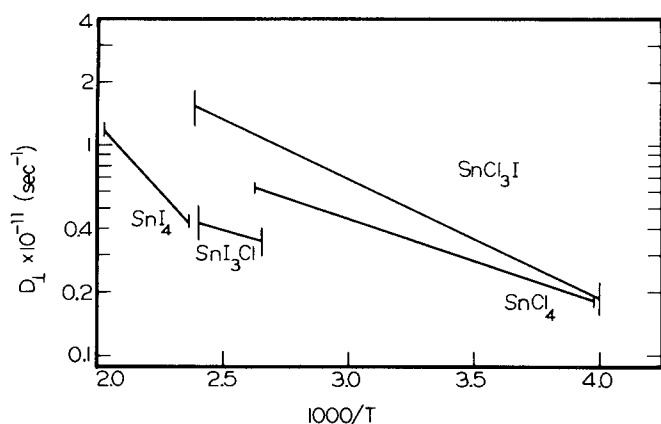


FIG. 6. Rotational diffusion coefficients for motion perpendicular to the threefold symmetry axes in tin chloriodides as a function of temperature.

orientation when large step angular displacements are important.

Rotational diffusion constants corresponding to motion of the threefold molecular axis have been computed for  $\text{SnI}_4$ ,  $\text{SnI}_3\text{Cl}$ ,  $\text{SnCl}_3\text{I}$ , and  $\text{SnCl}_4$  using measured relaxation times of the halogens on threefold axes and are plotted as a function of temperature in Fig. 6. Quadrupole coupling constants for  $\text{Sn}^{127}\text{I}_4$  and  $\text{Sn}^{35}\text{Cl}_4$  are taken from literature values of the NQR transitions.<sup>14,15</sup> NQR studies of the mixtures have not been undertaken, but fairly accurate quadrupole coupling constants can be computed using empirical substituent correlations derived by Semin and Bryuchova.<sup>16</sup> Their method employs "Taft-Hammett" parameters<sup>17</sup>  $\sigma_I$  and  $\sigma_C$  of the substituents to correlate changes in NQR frequencies according to the expression

$$(\nu - \nu_0)/\nu_0 = \sum \alpha_i \sigma_{ii} + \sum \beta_i \sigma_{Ci} \quad .$$

Semin and Bryuchova have correlated NQR frequencies of  $^{35}\text{Cl}$ ,  $^{81}\text{Br}$ , and  $^{127}\text{I}$  in about 150 tin compounds with typical accuracy of 0.5%–2.0%, the accuracy depending on the series of substituents correlated. Computed quadrupole coupling constants for  $\text{SnCl}_3\text{I}$  and  $\text{SnI}_3\text{Cl}$ , along with measured values for  $\text{SnI}_4$  and  $\text{SnCl}_4$ , are given in Table III. Substituent effects in the mixed chloriodides are seen to be very small, and it is believed that the error introduced by the correlation is less than 1%. However, quadrupole coupling constants of  $\text{SnBr}_4$  and  $\text{SnI}_4$  are slightly temperature dependent, decreasing by 2.5% as temperature is raised from 77 to 300° K, and a small but unknown change probably also occurs on melting. Since the correlation coefficients,  $\alpha$  and  $\beta$ , are derived from data at 77° K, computed coupling constants have been corrected upward by 2.5% to account partially for these effects. The coupling constants used contain a total estimated uncertainty of  $\pm 2\%$ . Absolute uncertainty in computed values of  $D_1$  is therefore essentially the same as that in the halogen  $T_1$ 's, and is approximately  $\pm 20\%$  for  $\text{SnCl}_3\text{I}$  and  $\text{SnI}_3\text{Cl}$ . Data for  $\text{SnI}_4$  and  $\text{SnCl}_4$  are taken from previous studies<sup>1</sup> on the neat liquids and are included for comparison. Uncertainty in  $D_1$  for these liquids is about  $\pm 7\%$ .

From a simple consideration of molecular shape it might be predicted that  $\text{SnI}_3\text{Cl}$  and  $\text{SnCl}_3\text{I}$ , which are substantially distorted tetrahedra, would experience greater resistance to reorientation of the unique axis than do the highly spherical molecules,  $\text{SnI}_4$  and  $\text{SnCl}_4$ . The existence of large dipole moments in the mixed species also inhibits reorientation of the unique axis by producing a tendency toward short range dipolar alignment of neighboring molecules in the liquid phase. Measured values of  $D_1$  lengthen in a fairly regular manner as the number of chlorines are increased, however, indicating that these shape and symmetry factors are not the most important determinants of intermolecular frictional coefficients. In a previous study, Rothschild has similarly observed the relative insignificance of dipolar forces on reorientational motion of methylene chloride.<sup>18</sup> The most likely explanation for the slow and regular variation of  $D_1$  in Fig. 6 is that intermolecular friction is closely related to the magnitude of London dispersion forces. Stronger intermolecular attractive forces lead to tighter molecular packing and consequently to greater rotational friction. Steele<sup>12</sup> and Huntress<sup>10</sup> have derived a formal relation between the rotation diffusion constant and angular gradients of the intermolecular potential energy function  $U(\mathbf{R}^N)$ ,

$$\zeta = \frac{kT}{D} = \left[ \frac{2I}{\pi} \left\langle \frac{\partial^2 U(\mathbf{R}^N)}{\partial \theta^2} \right\rangle \right]^{1/2};$$

$\zeta$  is the rotational friction constant in Steele's model. Dispersion forces largely determine the absolute magnitude of  $U(\mathbf{R}^N)$  in the liquids discussed here. The profound effect of London dispersion on intermolecular attraction is mirrored in the steady rise of melting and boiling points for the covalent tin tetrahalides:

	$\text{SnCl}_4$	$\text{SnBr}_4$	$\text{SnI}_4$
mp(° C)	-33	31	145
bp(° C)	114	202	365

London dispersion will strongly influence the angular gradients of  $U(\mathbf{R}^N)$  through tighter molecular packing even though the attractive force itself possesses spherical symmetry. Very large dispersion forces must be responsible for the small measured rotational diffusion constant of  $\text{SnI}_4$ , which is highly spherical and lacks electric dipole and quadrupole moments. An unqualified correlation of rotational diffusion coefficients with dispersion forces may be misleading however, since  $\text{SnBr}_4$  appears to reorient more rapidly than either  $\text{SnCl}_4$  or  $\text{SnI}_4$  at a given temperature.<sup>1</sup>

When comparing molecular motion in different liquids and liquid mixtures, it is necessary to assess the dependence of  $D_1$  on the composition of the mixture. This may be done very simply for  $\text{SnCl}_4$  and  $\text{SnI}_4$  by comparing  $^{119}\text{Sn}$  relaxation times in the liquid mixtures with  $T_1$ 's previously measured in the neat liquids. Data for  $\text{SnCl}_4$  in the neat liquid is essentially identical to data from the mixtures, indicating that solvent effects on the molecular motion of  $\text{SnCl}_4$  are quite small. On the other hand the  $T_1$ 's of  $\text{SnI}_4$  appear to undergo a slight systematic shortening of about 7% in the 3:1 mixture as shown in Fig. 7. The relatively small influence of composition on rotational diffusion is not unexpected since the mix-

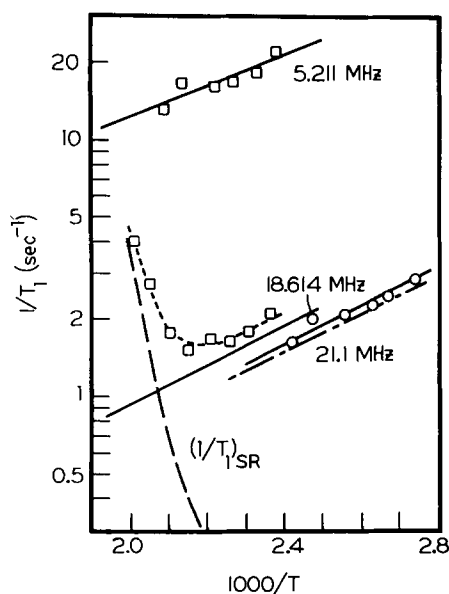


FIG. 7. Comparison of spin-lattice relaxation for  $^{119}\text{SnI}_4$  in the neat liquid ( $\square$ ) and in a 3:1  $\text{SnI}_4/\text{SnCl}_4$  mixture ( $\circ$ ). The dashed line shows where data from the mixture should fall if there were no medium effects.

tures studied contain about 75% of  $\text{SnX}_4$  and  $\text{SnX}_3\text{Y}$ , and less than 25% of other species. Dispersion forces, as well as experimental values of  $D_{\perp}$ , are quite similar for the dominant pairs in the mixtures ( $\text{SnI}_4$ ,  $\text{SnI}_3\text{Cl}$ ) and ( $\text{SnCl}_3\text{I}$ ,  $\text{SnCl}_4$ ). Since electric dipole moments and departures from tetrahedral symmetry have relatively little effect on reorientational motion, and since dispersion forces are similar for dominant molecular species in the mixtures, the observed insensitivity of  $D_{\perp}$  to changes in the composition of the medium is not surprising.

Diffusion coefficients  $D_{\parallel}$ , for motion about the unique axis can also be computed by combining relaxation data for the on- and off-axis halogen nuclei. Shimizu<sup>9</sup> and Huntress<sup>10</sup> have shown that the relaxation rate of an off-axis quadrupole nucleus is given (in the "decoupled" rotor approximation) by

$$(T_2)^{-1} = \frac{1}{80} \left[ \frac{2I+3}{I^2(2I-1)} \right] \times \frac{(e^2qQ/\hbar)^2}{D_{\perp}} \left\{ 1 + \frac{(D_{\perp} - D_{\parallel})}{(D_{\perp} + D_{\parallel})} \sin^2\theta \right\}.$$

$D_{\perp}$  can be obtained independently from a second, on-axis, resonance using Eq. (5). This calculation has been carried out for  $\text{SnI}_3\text{Cl}$ , for which both  $^{127}\text{I}$  and  $^{35}\text{Cl}$  relaxation times have been measured. The computed ratio,  $D_{\perp}/D_{\parallel} = 1.27 \pm 0.40$  at 400°K, indicates that the anisotropy of rotational motion is fairly small and is within the uncertainty of our measurements. The lack of large anisotropy in the rotational diffusion tensor is consistent with a relatively small influence of shape factors and electric dipole moments on reorientational diffusion.

## CONCLUSIONS

A growing body of experimental data indicates that the kinds of information obtainable from relaxation times of

spin- $\frac{1}{2}$  isotopes of heavy elements (e.g.,  $^{117,119}\text{Sn}$ ,  $^{207}\text{Pb}$ ,  $^{203,205}\text{Tl}$ ,  $^{111,113}\text{Cd}$ ,  $^{119}\text{Hg}$ ,  $^{77}\text{Se}$ ,  $^{123,125}\text{Te}$ ,  $^{107,109}\text{Ag}$ , and  $^{195}\text{Pt}$ ) differs significantly from that commonly obtained from lighter nuclei. Nuclear dipole interactions are relatively much less important as relaxation mechanisms for the heavy isotopes, while spin-rotation coupling provides an increasingly efficient relaxation pathway. Mechanistic investigations of  $T_1$  in a wide variety of organometallic compounds of lead,<sup>19,20</sup> tin<sup>7</sup> and cadmium<sup>21,22</sup> have shown that spin-rotation dominates relaxation throughout the liquid range and that dipolar relaxation is very small, usually below the limits of detection. The present experiments, and others in this series,<sup>1,23</sup> show that Abragam's "scalar relaxation of the second kind"<sup>2</sup> can also become a very efficient  $T_1$  mechanism when the heavy metal is directly bonded to bromine or iodine. The efficiency of this mechanism decreases as the square of the magnetic field strength, but relative to spin-rotation, scalar coupling can be a highly efficient relaxation mechanism even at 25 kG. Our data on  $\text{SnICl}_3$  demonstrates that scalar coupling dominates spin-rotation over much of the liquid range even though only one iodine contributes to the scalar coupling and the relaxation time of the iodine is relatively long.  $(T_1)_{\text{SC}}^{-1}$  is inversely proportional to the halogen relaxation time, and thus is directly proportional to molecular rotational correlation times. Metal iodides and bromides that are bulkier or less spherical than the quasi-tetrahedral molecules studied here can therefore be expected to exhibit even more efficient scalar relaxation due to their longer correlation times and shorter halogen  $T_2$ 's.

Whenever scalar coupling provides a dominant relaxation pathway for  $T_1$ , it will also dominate  $T_2$ . By measuring both  $T_1$  and  $T_2$  it should be possible to measure routinely halogen spin-spin coupling constants and relaxation times in many metal bromides and iodides. These measurements will not in general be possible when more than one kind of halogen is bonded to the metal however, since  $T_1$  and  $T_2$  will in nearly all cases be dominated by different halogens. The present work demonstrates the feasibility of measuring coupling constants and very short relaxation times from  $T_1$  data alone by using low field measurements, where  $(T_1)_{\text{SC}}^{-1}$  passes through a maximum.

Due to the very large chemical shift ranges of heavy isotopes we at first expected that chemical shift anisotropy would provide a significant  $T_1$  pathway for the heavy metals. No such contribution was found for  $\text{SnI}_3\text{Cl}$  or  $\text{SnCl}_3\text{I}$  at 13.3 kG, even though the shielding anisotropy is probably very large (> 1000 ppm) for these molecules relative to other tin compounds. A review of chemical shift anisotropies shows that they usually have a similar magnitude to the range of chemical shifts of a given nucleus.<sup>24</sup> The chemical shift between  $\text{SnCl}_4$  and  $\text{SnI}_4$  is very large (1548 ppm) on the scale of known  $^{119}\text{Sn}$  shifts, thus suggesting a large anisotropy. However the presence of  $^{127}\text{I}$  produces a very efficient scalar component to  $T_1$  which serves to mask other mechanisms that have the same temperature dependence. Furthermore,  $(T_1)_{\text{CSA}}^{-1}$  increases as the square of the field strength, and it is quite possible that it may become detectable in tin



compounds at 25 kG and even dominant at superconductive fields.

#### ACKNOWLEDGMENTS

We wish to acknowledge financial support for this research from the National Science Foundation. One of us (J. W. T.) received support in the form of a fellowship from the Ethyl Corporation.

\*Present address: Merck, Sharp and Dohme Co., Rahway, NJ.

- <sup>1</sup>R. R. Sharp, *J. Chem. Phys.* **57**, 5321 (1972); **60**, 1149 (1974).  
<sup>2</sup>A. Abragam, *Principles of Magnetic Resonance* (Oxford, London, 1961), Chap. VIII.  
<sup>3</sup>M. L. Delwaulle, M. B. Buisset, and M. Delhay, *J. Phys. Chem.* **74**, 5768 (1952).  
<sup>4</sup>C. Cerf, *Bull. Soc. Chim. Fr.* **8**, 2889 (1971).  
<sup>5</sup>J. J. Burke and P. C. Lauterbur, *J. Am. Chem. Soc.* **83**, 326 (1960).  
<sup>6</sup>R. M. Hawk, R. R. Sharp, and J. W. Tolan, *Rev. Sci. Instrum.* **45**, 96 (1974).  
<sup>7</sup>C. Lassigne, Ph.D. thesis, Simon Fraser University, 1975.  
<sup>8</sup>K. J. Johnson, J. P. Hunt, and H. W. Dodgen, *J. Chem. Phys.* **51**, 4493 (1969).

- <sup>9</sup>H. Shimizu, *J. Chem. Phys.* **40**, 754 (1964).  
<sup>10</sup>W. T. Huntress, Jr., *Adv. Magn. Reson.* **4**, 1 (1970).  
<sup>11</sup>P. S. Hubbard, *Phys. Rev.* **131**, 1155 (1963).  
<sup>12</sup>W. A. Steele, *J. Chem. Phys.*, **38**, 2404, 2411 (1963).  
<sup>13</sup>R. E. D. McClung, *J. Chem. Phys.* **51**, 3142 (1969); R. G. Gordon, *J. Chem. Phys.* **44**, 1830 (1966).  
<sup>14</sup>I. P. Biryukov, M. G. Voronkov, and I. A. Safin, *Tables of N. Q. R. Resonance Frequencies* (Israel Program for Scientific Translations, Jerusalem, 1969).  
<sup>15</sup>K. Shimomura, *J. Sci. Hiroshima Univ. Ser. A: Phys. Chem.* **17**, 383 (1954).  
<sup>16</sup>G. K. Semin and E. V. Bryuchova, *Chem. Commun.* 1968, 605.  
<sup>17</sup>R. V. Taft, in *Steric Effects in Organic Chemistry*, edited by M. S. Newman (Wiley, New York, 1965).  
<sup>18</sup>W. G. Rothschild, *J. Chem. Phys.* **53**, 990 (1970).  
<sup>19</sup>G. E. Macieland, J. L. Dallas, *J. Am. Chem. Soc.* **95**, 3039 (1973).  
<sup>20</sup>R. M. Hawk, Ph.D. thesis, University of Michigan, 1973.  
<sup>21</sup>A. D. Cardin, P. D. Ellis, J. D. Odom, and J. W. Howard, Jr., *J. Am. Chem. Soc.* **97**, 1672 (1975).  
<sup>22</sup>J. W. Tolan, Ph.D. thesis University of Michigan, 1974).  
<sup>23</sup>R. M. Hawk and R. R. Sharp, *J. Chem. Phys.* **60**, 1009 (1974).  
<sup>24</sup>B. R. Appleman and B. P. Dailey, *Adv. Magn. Reson.* **7**, 231 (1974).  
<sup>25</sup>Gmelin-Institut, *Gmelins Handbuch der Anorganischen Chemie* Teil C1, (Chemie, Weinheim, 1972), Pt. C1, pp. 437 ff.